

Lawrence Berkeley National Laboratory

Recent Work

Title

A MACROSCOPIC-IMPEDANCE MODEL FOR A ROTATING-DISK ELECTRODE

Permalink

<https://escholarship.org/uc/item/2f99d9zj>

Authors

Hauser, A.K.
Newman, J.

Publication Date

1989-03-01



Lawrence Berkeley Laboratory

UNIVERSITY OF CALIFORNIA

Materials & Chemical Sciences Division

RECEIVED
LAWRENCE
BERKELEY LABORATORY

JUL 3 1989

Submitted to Journal of the Electrochemical Society

LIBRARY AND
DOCUMENTS SECTION

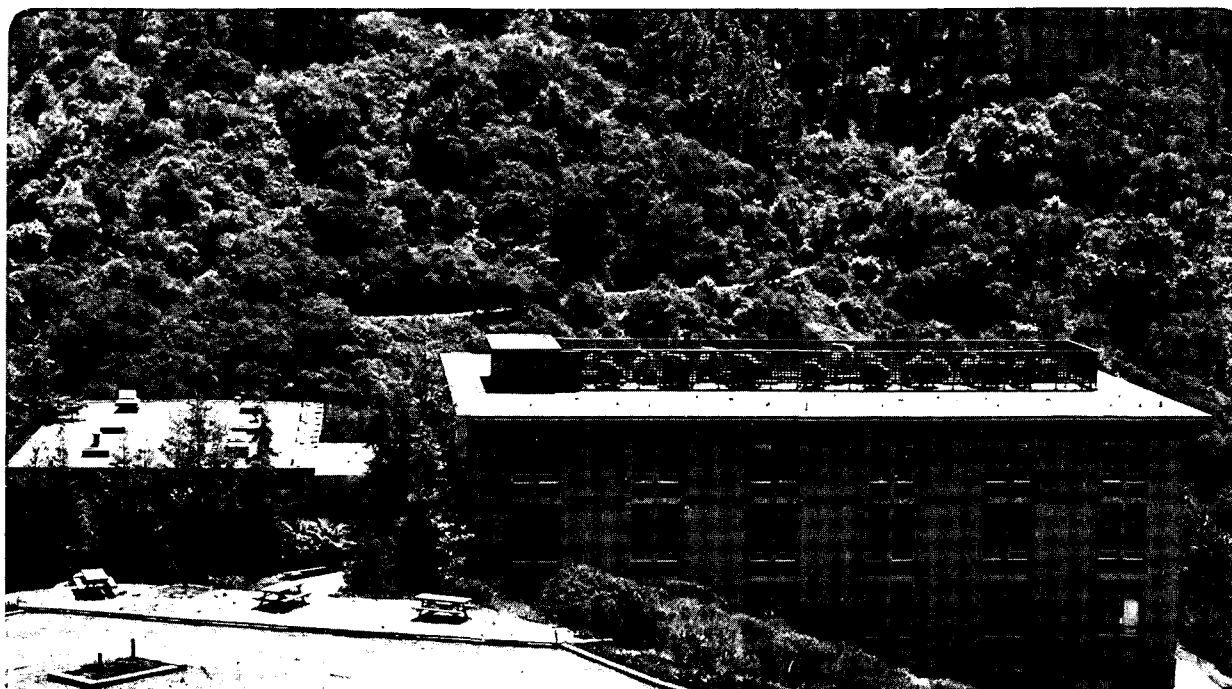
A Macroscopic-Impedance Model for a Rotating-Disk Electrode

A.K. Hauser and J. Newman

March 1989

For Reference

Not to be taken from this room



LBL-26267
c.1

DISCLAIMER

This document was prepared as an account of work sponsored by the United States Government. While this document is believed to contain correct information, neither the United States Government nor any agency thereof, nor the Regents of the University of California, nor any of their employees, makes any warranty, express or implied, or assumes any legal responsibility for the accuracy, completeness, or usefulness of any information, apparatus, product, or process disclosed, or represents that its use would not infringe privately owned rights. Reference herein to any specific commercial product, process, or service by its trade name, trademark, manufacturer, or otherwise, does not necessarily constitute or imply its endorsement, recommendation, or favoring by the United States Government or any agency thereof, or the Regents of the University of California. The views and opinions of authors expressed herein do not necessarily state or reflect those of the United States Government or any agency thereof or the Regents of the University of California.

LBL-26267

A Macroscopic-Impedance Model for a Rotating-Disk Electrode

Alan K. Hauser and John Newman

Department of Chemical Engineering
University of California

and

Materials and Chemical Sciences Division
Lawrence Berkeley Laboratory
One Cyclotron Road
Berkeley, CA 94720

March 21, 1989

A Macroscopic-Impedance Model for a Rotating-Disk Electrode

Alan K. Hauser and John Newman

Department of Chemical Engineering, University of California, and
Materials and Chemical Sciences Division, Lawrence Berkeley Laboratory,
One Cyclotron Road, Berkeley, CA 94720

March 18, 1989

Abstract

A mathematical model is presented that can calculate the frequency response of a rotating disk accounting for multicomponent diffusion, migration, and homogeneous and heterogeneous reactions. The working algorithm uses concentrated-solution theory, incorporating the Stefan-Maxwell transport equations, and accounts for a finite Schmidt number and interfacial velocity. The governing equations of the disk boundary layer and electrode boundary condition are first discussed. Next, the electrochemical impedance of the disk electrode is analyzed theoretically. This includes examining the impedance due to each contribution of the total cell potential and total current. This is necessary because the definitions of some terms used in the electrochemical impedance literature are often confusing and not universally recognized. Such a fundamental approach of formulating the problem gives rise to impedance terms typically neglected in other ac-impedance treatments.

key words: Stefan-Maxwell multicomponent transport, faradaic impedance

1. Introduction

A mathematical treatment of the total electrochemical impedance of a rotating disk electrode is to be presented. The macroscopic model[†] utilizes the Stefan-Maxwell multicomponent transport equations to describe diffusion and migration in concentrated solutions with homogeneous chemical and heterogeneous electrode reactions. This model is capable of predicting the impedance behavior for many electrochemical systems, although in this paper, only the governing equations are discussed. In later papers, the developed model will be applied to the anodic dissolution of copper in chloride solutions.

2. Model Development

The macroscopic model to be presented has been discussed^[1] previously. Therefore, details of concentrated-solution theory will not be described here. Instead, an overview of the equations, boundary equations, and numerical procedure will be given with emphasis on the new contributions to the model and to formulation of the impedance problem in general.

2.1. Governing Equations

The Stefan-Maxwell transport equations to be outlined account for multicomponent concentrated-solution theory,^[2] including migration, diffusion, convection, and homogeneous reaction kinetics within the mass-transfer boundary layer.

[†] Macroscopic refers to the rotating-disk boundary layer, as opposed to a microscopic double-layer model.

The generalized set of governing equations in the distributed, macroscopic model is summarized in table 1. There are $2n + 1$ variables and equations in the model, where n is the number of species present, including the solvent. The variables: electrostatic potential Φ , mole fractions, x_0 for the solvent and $x_i = c_i/c_T$ for species i , and the molar fluxes, J_0 and $J_i = c_i(v_i - v)$ relative to the mass-average velocity v , are functions of the axial distance z from the electrode and of time.

In matching variables and equations, the first three equations in table 1, the electroneutrality equation, the mole fraction relationship, and the molar flux/molecular

Table 1. Governing equations in the distributed macroscopic model.

<i>Variables</i>	<i>Equations</i>	<i>Number</i>
$\Phi(z)$	$\sum_i z_i x_i = 0$	1
$x_0(z)$	$\sum_i x_i = 1$	1
$J_0(z)$	$\sum_i M_i J_i = 0$	1
$J_i(z)$	$\nabla x_i + \frac{z_i F}{RT} x_i \nabla \Phi = \sum_{k \neq i} \frac{x_i J_k - x_k J_i}{c_T D_{i,k}}$	$n - 1$
$x_i(z)$	$\frac{\partial c_i}{\partial t} = -\nabla \cdot J_i + R_i - c_T \mathbf{v} \cdot \nabla x_i + c_i \mathbf{v} \cdot \nabla \ln \bar{M}$	$n - 1$
		$2n + 1$

weight relationship, can correspond to the electrostatic potential and the solvent mole fraction and flux. The remaining $n - 1$ transport equations and $n - 1$ material balances are for the $2n - 2$ mole fractions and fluxes. M_i is the molecular weight of species i , and \bar{M} is the average molecular weight of the solution, weighted by mole fractions and including the solvent. R_i is rate of homogeneous production, and our treatment of chemical-reaction kinetics is summarized in table 2. The first equation in the table represents a single homogeneous reaction. Activity coefficients are not accounted for in the model at this time but can be added without disrupting the calculation scheme.

$D_{i,k}$ is the concentrated-solution-theory diffusion coefficient describing the interaction of species i and k . The number of transport properties defined by the Stefan-Maxwell equation is $\frac{1}{2}n(n - 1)$, since $D_{i,k} = D_{k,i}$ and $D_{i,i}$ is not defined. It should be noted that these transport properties are rigorously to be obtained from independent measurements of the conductivity, $(n - 2)$ transference numbers, and $\frac{1}{2}(n - 1)(n - 2)$ diffusion coefficients corresponding to interdiffusion of neutral combinations of species. Thus, for four species (for example, three ions and a solvent) there are six transport properties: six coefficients $D_{j,k}$ corresponding to one conductivity, two independent transference numbers, and three diffusion coefficients required to describe diffusion of the electrolyte c_B and supporting electrolyte c_A in the solvent.

Table 2. Homogeneous-reaction equations[†] used in the concentrated-solution model.

$$\sum_i \nu_{i,l} M_i^z \rightarrow 0$$

$$R_l = - \sum_i \nu_{i,l} \hat{R}_l$$

$$\hat{R}_l = \hat{k}_{b,l} \left[\hat{K}_{c,l} \prod_i c_i^{\nu_{i,l}} - \prod_i c_i^{-\nu_{i,l}} \right]$$

$$\nu_{i,l} > 0 \quad \nu_{i,l} < 0$$

$$\hat{K}_{c,l} = \frac{\hat{k}_{f,l}}{\hat{k}_{b,l}} = \prod_i c_i^{-\nu_{i,l}} = \hat{K}_l (\rho_0')^{-\nu_l}$$

$$\ln \hat{K}_l = \frac{1}{RT} \sum_i \nu_{i,l} \mu_i^\theta, \quad \nu_l = \sum_i \nu_{i,l}$$

Rotating-Disk Electrode

A particular geometry must be specified before the mass-transfer governing equations in table 1 can be solved. For this work, the rotating disk has been chosen,

[†] It should be noted that nonconventional chemistry notation is being used here since $\nu_{i,l}$ is positive for reactants, instead of being positive for products. Therefore, $\Delta G_l^\theta = - \sum_i \nu_{i,l} \mu_i^\theta$ instead of $\Delta G_l^\theta = \sum_i \nu_{i,l} \mu_i^\theta$. This is done so that the stoichiometry of the electrochemical and chemical reactions is consistent.

because its hydrodynamics^{[3], [4], [5]} are well known and it has good mass-transfer properties,^{[6], [7]} such as providing an uniformly accessible surface. Additionally, the degree of nonuniformity of the current distribution^[8] and the frequency dispersion in impedance measurements,^[9] both due to ohmic effects, have been assessed.

Next, we briefly discuss the characterization of the diffusion layer near a rotating disk, first under steady-state conditions, followed by a discussion of the frequency dependence of the concentration profiles. Concentration variations in the boundary layer are created by the electrode-reaction processes, which lead to depletion of the solution near the cathode and an enhancement of the concentration near the anode. Diffusion is important in the thin region adjacent to the disk because the axial velocity is small. Further from the electrode however, forced convection becomes the dominating mode of transport because of the high rates of stirring due to rotation of the disk.

The effect of mass transfer due to convection is characterized by the equations for the rotating disk given in table 3. The normal component of the velocity for short distances from the disk is expressed as a dimensionless power series as a function of ζ , the dimensionless variable used in the Von Kármán transformation.^[3] The dimensionless interfacial velocity, $H(0)$, is included, where r_l is the rate of the heterogeneous reaction l and will be discussed in the next section. The equations in table 3 are restricted to constant fluid density and viscosity, whereas the equations in table 1 are not. Therefore, if physical-property data were available, variable fluid properties could be accounted for. The method of handling the coupled hydrodynamic and mass-transport problem in concentrated solutions with variable physical properties

Table 3. Supplementary equations used in the concentrated-solution model.Scaling of the Boundary Layer

$$z_{\max} = \xi_{\max} \left(\frac{3D_R}{a\nu} \right)^{1/3} \left(\frac{\nu}{\Omega} \right)^{1/2}$$

$$\frac{1}{\xi_{\max}} = \frac{\left(D_R / D_{\max} \right)^{1/3}}{2.0} + \frac{\left(pSc^{1/3} \right)^{1/2}}{5.4}$$

RDE Velocity Profiles

$$v_z = (\nu\Omega)^{1/2} H(\zeta) \quad , \quad \text{where} \quad \zeta = z \left(\frac{\Omega}{\nu} \right)^{1/2}$$

$$H(\zeta) = H(0) - a \zeta^2 + \frac{1}{3} \zeta^3 + \frac{b}{6} \zeta^4 + \frac{b^2}{30} \zeta^5 + \frac{a}{180} \zeta^6 - \frac{(1-4ab)}{1260} \zeta^7$$

$$H(0) = \frac{-1}{c_T \bar{M} (\nu\Omega)^{1/2}} \sum_i M_i \sum_l s_{i,l} r_l \quad , \quad \text{where} \quad \bar{M} = \sum_i x_i M_i$$

is well worked out.^{[10], [11]}

For the transient mass-transfer problem, the concentration of ions responds to the sinusoidal ac perturbation at the surface, and then the concentration fluctuations propagate from the electrode out into the solution until eventually the concentration wave is completely damped out. The frequency dependence of the depth of penetration

of the ac-concentration variations was cited by Vetter,^[12] where it was shown that the ac diffusion-layer thickness (the Warburg line) varies inversely with the square root of the frequency, *i.e.*, $\delta_i(\omega) \propto \sqrt{D_i/\omega}$. Thus, the ratio of $\delta_i(\omega)$ to the steady-state, Nernst diffusion-layer thickness (given by the Levich equation: $\bar{\delta}_i = 1.6117 D_i^{1/3} \nu^{1/6} \Omega^{-1/2}$), yields the frequency-dependent mass-transfer function $(pSc^{1/3})^{-1/2}$, where $p = \omega/\Omega$ is the dimensionless perturbation frequency and $Sc = \nu/D_R$ is the Schmidt number of the reference species.

It is well known that the rotating-disk problem can be properly scaled using the dimensionless parameter $\xi = z(\Omega/\nu)^{1/2} (a\nu/3D_R)^{1/3}$, arising from the dimensionless convective-diffusion equation.^[2] For computational convenience, we introduce a boundary-layer thickness z_{\max} , such that the diffusion-layer is always within the somewhat arbitrarily chosen z_{\max} . The frequency-dependent nature of the diffusion layer thickness was alluded to above, and therefore justifies our introduction of the dimensionless maximum distance from the disk, ξ_{\max} , given in table 3. In the steady state, $\xi_{\max} = 2 (D_{\max}/D_R)^{1/3}$, where the diffusion-layer thickness is scaled based on the largest diffusion coefficient in the problem, D_{\max} .

2.2. Boundary Conditions

Before the problem can be resolved, the corresponding boundary conditions must be specified. The mathematical formulation of the governing equations at the boundaries is given in table 4. Far from the disk, the composition approaches that of the bulk fluid, and the potential is arbitrarily set to zero at the position ξ_{\max} . The interface, where multiple charge-transfer reactions can occur, serves as the other

Table 4. Governing equations at the boundaries used in the concentrated-solution model.

<u>Electrode Surface</u>		
$\frac{\partial \Gamma_{i,d}}{\partial t} = N_i^{(ct)} - N_i(\xi = 0)$		$n - 1$
$\Gamma_{i,d} = \frac{-z_i c_{i,0} C_{M-2} V}{F \sum_j z_j^2 c_{j,0}}$		
$\sum_i z_i x_i = 0$		1
<u>Bulk Solution</u>		
$x_i = x_{i,\infty}$ at $\xi = \infty$		$n - 1$
$\Phi = 0$ at $\xi = \xi_{\max}$		1

boundary. At steady state, the first equation in table 4 reduces to $N_i^{(ct)} = c_{i,0} v_0 + J_i(\xi = 0)$, where the molar flux $N_i(\xi = 0)$ at the electrode is expressed in terms of the velocity through the interface, v_0 , and the flux, J_i , calculated relative to the mass-average velocity. For nonsteady-state conditions, diffuse-layer adsorption is important. Thus, the surface excess $\Gamma_{i,d}$ of all ionic species in the diffuse part of the double layer must be accounted for using the transient material balance in table 4. Linearized diffuse-layer theory (see appendix A) can be applied, yielding the second equation in table 4. On the solution side of the interface, the electroneutrality condition

remains valid up to the inner limit of the diffusion layer, although, strictly speaking, it is not a boundary condition.

A single electrochemical reaction is represented by



and the modified Butler-Volmer expression given in table 5 describes its kinetics, when the reaction order is assumed to be proportional to the reaction's stoichiometry. $V = \Phi_m - \Phi_0$ is the electrode potential minus the potential of a reference electrode of a given kind located just outside the diffuse part of the double layer. The reference electrode of a given kind has been chosen to be the saturated calomel electrode in the equations. This potential difference serves as the kinetic driving force for the faradaic charge-transfer reactions. The kinetic relationship, along with equations for the equilibrium constants also given in table 5, completes the set of governing equations for the macroscopic transport model.

2.3. Breakdown of V_{tot}

Next, we should express the theoretical kinetic potential difference, V , in terms of the measurable cell potential, $V_{tot} = \Phi_m - \Phi_{RR}$. V_{tot} is the electrode potential relative to a real reference electrode located in the bulk solution, essentially at infinity. The total cell potential will be used later in the determination of the total electrochemical impedance and may be rewritten[†]

[†] An alternative breakdown of V_{tot} in terms of the more commonly used surface and concentration overpotentials is given in appendix B.

Table 5. Supplementary equations describing the faradaic reactions.

$$N_i^{(ct)} = - \sum_l s_{i,l} r_l = - \sum_l \frac{s_{i,l}}{n_l F} i_{f,l} , \quad n_l = - \sum_i s_{i,l} z_i$$

$$r_l = k_{b,l} \left[\begin{array}{cc} K_{c,l} \exp \left((1-\beta_l) \frac{n_l F}{RT} V \right) \prod_i c_{i,0}^{s_{i,l}} & - \exp \left(-\beta_l \frac{n_l F}{RT} V \right) \prod_i c_{i,0}^{-s_{i,l}} \\ s_{i,l} > 0 & s_{i,l} < 0 \end{array} \right]$$

$$K_{c,l} = \frac{k_{f,l}}{k_{b,l}} = K_l \left[\rho_0' \right]^{-s_l} , \quad s_l = \sum_i s_{i,l}$$

$$K_l = \left(\frac{\rho_0'}{c_{Cl^-,sat}} \right)^{n_l} \exp \left(- \frac{n_l F}{RT} U_{l/RG}^\theta \right)$$

$$FU_l^\theta = \frac{1}{2} \mu_{H_2}^* - \mu_{H^+}^\theta - \frac{1}{n_l} \sum_i s_{i,l} \mu_i^\theta , \quad U_{l/RG}^\theta = U_l^\theta - U_{RG}^\theta$$

$$V_{tot} = (\Phi_m - \Phi_0) + (\Phi_0 - \Phi_b) + (\Phi_b - \Phi_{RR}) , \quad (2)$$

where the first term on the right is the potential difference of interest, V . The final term reduces to the liquid junction potential, $\Delta\Phi_{LJ}$, if the reference electrodes of a given and a real kind are chosen to be the same. $\Delta\Phi_{LJ}$ depends on how the junction is formed and the concentration profile. The Henderson formula^[13] may be used for a continuous-mixture junction; however, this difference is quite small in practice, and usually can be neglected. Furthermore, it is not part of the impedance problem.

The second term contains an ohmic contribution and the diffusion potential and takes the form^[2]

$$\Phi_0 - \Phi_b = \int_0^b \frac{i}{\kappa} dz + \frac{RT}{F} \int_0^b \sum_j \frac{t_j^0}{z_j} \frac{\partial \ln(c_j f_{j,n})}{\partial z} dz \quad , \quad (3)$$

where t_j^0 is the transference number of species j with respect to the velocity of the solvent, $f_{j,n} = f_j / f_n^{z_j/z_n}$ is the molar activity coefficient of species j relative to the reference species n , and κ is the electrolytic conductivity, a well-recognized physical property given in reference 2 for concentrated solutions or for dilute solutions by

$$\kappa = \frac{F^2}{RT} \sum_i z_i^2 D_i c_i \quad . \quad (4)$$

Activity coefficients would need to be introduced into the treatment of multicomponent transport for greater rigor, as was done in reference 10 for a binary solution. The lack of a general data base for multicomponent solutions hampers this effort of applying concentrated-solution theory (see also Smyrl and Newman^[14] and chapters 4 and 6 of reference [2]).

The potential difference between the solution adjacent to the electrode surface and a hemispherical counterelectrode located at infinity can be expressed in terms of the well-known ohmic resistance^[15] for a primary current distribution to a disk, $(4\kappa_\infty r_0)^{-1}$, by using the following:

$$\Phi_0 - \Phi_b = (\Phi_0 - \hat{\Phi}_0) + (\hat{\Phi}_0 - \Phi_b) \quad . \quad (5)$$

$\hat{\Phi}_0$ is the potential of the solution just outside the diffuse layer which would be determined by a reference electrode of a given kind if there were no concentration gradients across the boundary layer, but the same current distribution prevailed. The second term on the right in equation 5 is the ohmic potential drop between the surface

and the bulk calculated using Laplace's equation, assuming the conductivity is constant and equal to the bulk solution value, κ_∞ . Thus, the ohmic-potential term is given by

$$\Delta\hat{\Phi}_{ohm} = \hat{\Phi}_0 - \Phi_b = i \frac{\pi r_0}{4\kappa_\infty} = i R_\Omega \quad , \quad (6)$$

where i is related to the total current, $I = \pi r_0^2 i$, and R_Ω is in $\text{ohm}\cdot\text{cm}^2$. Finally, a breakdown of the total cell potential is illustrated schematically in figure 1, and equation 2 can be rewritten

$$V_{tot} = V + (\Phi_0 - \hat{\Phi}_0) + i R_\Omega + \Delta\Phi_{LJ} \quad , \quad (7)$$

and will be used later to yield the total electrochemical impedance. Use of a primary resistance value for R_Ω ignores the realities of a nonuniform current distribution on the disk electrode.^[8,9]

3. Electrochemical Impedance Determination

The governing equations, boundary conditions, and a detailed breakdown of the total cell potential have been presented that fully specify the kinetic and transport problem to a rotating disk in concentrated solutions. Once the concentration and potential profiles are determined, the current can be calculated using a linear-response-analysis, which then allows the electrochemical impedance to be predicted. Let us next briefly review the linear-response analysis procedure and then discuss the numerical procedure that is used to solve the macroscopic impedance problem.

3.1. Linear-Response Analysis

A linear-response analysis is used here to determine the total impedance. A linear response is accomplished experimentally by applying a small perturbation signal about a

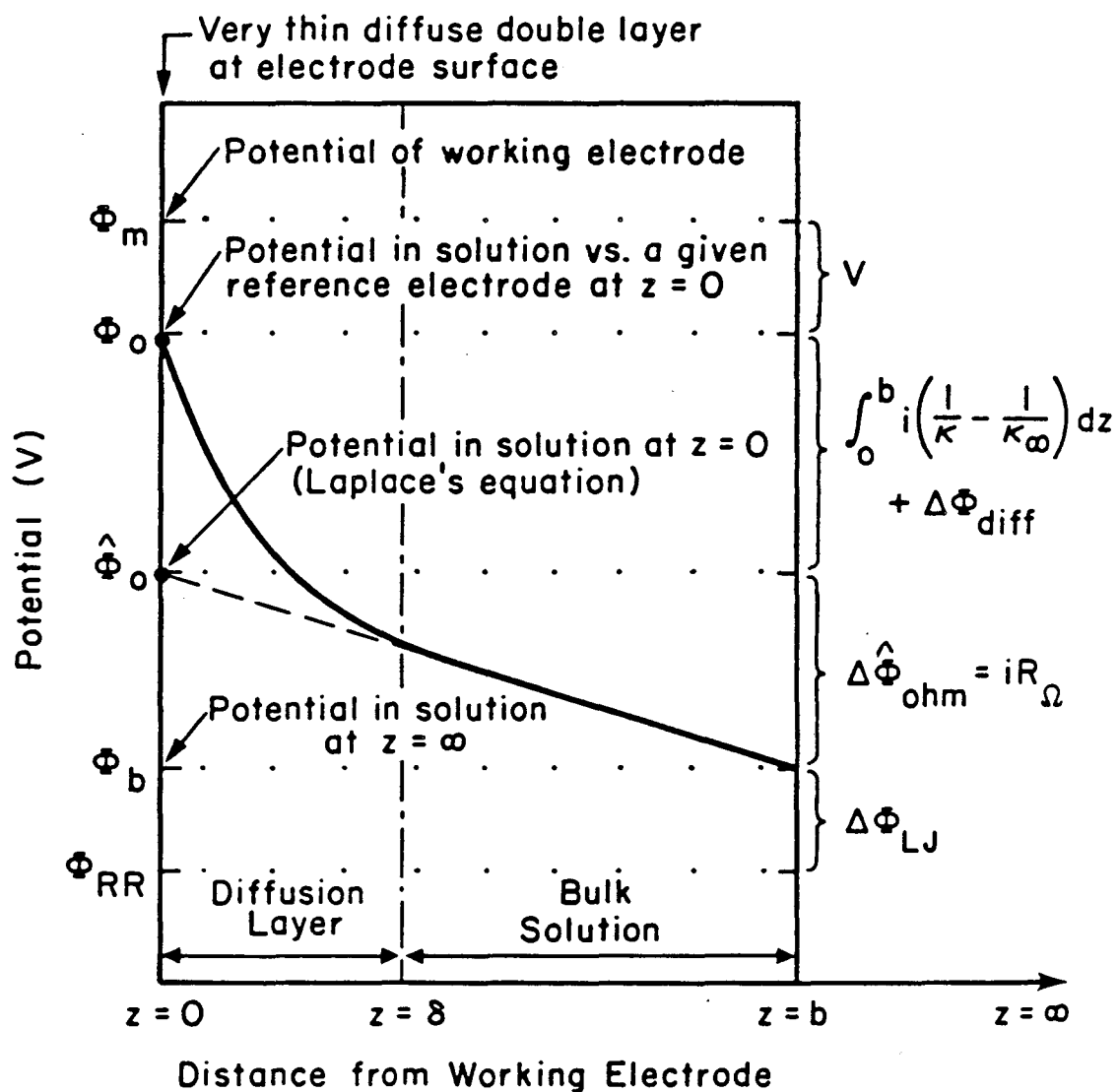


Figure 1. Breakdown of V_{tot} into a number of tractable components.

steady-state polarization point (\bar{V}_{tot}, \bar{i}) . The electrochemical system of interest is disturbed by superimposing a low amplitude alternating-potential perturbation, $\delta V_{tot} = |V_{tot}| \cos(\omega t)$, of frequency ω onto a steady-state potential, \bar{V} . The system responds to this sinusoidal-potential by relaxing to a new pseudo-steady state. The small alternating-current output, $\tilde{i} = |\tilde{i}| \cos(\omega t - \phi)$, will be at the same frequency of perturbation, but will be phase shifted and have an amplitude different from the input signal.

The total impedance Z_{tot} of the electrochemical system is the ratio of the alternating voltage to the current response and is given by

$$Z_{tot} = \frac{\tilde{V}_{tot}}{\tilde{i}} = |Z_{tot}| \exp(j\phi) = \text{Re} \{ Z_{tot} \} + j \text{Im} \{ Z_{tot} \} \quad (8)$$

when phasor notation is used. The magnitude of the total impedance

$$|Z_{tot}| = \frac{|\tilde{V}_{tot}|}{|\tilde{i}|} = \sqrt{\text{Re} \{ Z_{tot} \}^2 + \text{Im} \{ Z_{tot} \}^2} \quad (9)$$

is expressed in $\text{ohm}\cdot\text{cm}^2$, and the phase shift between the current and the potential is given by $\phi = \arctan(\text{Im} \{ Z_{tot} \} / \text{Re} \{ Z_{tot} \})$.

3.2. Computational Procedure

Each variable in the problem, concentrations of all the species and the potential, takes the form[†] of $\chi = \bar{\chi} + \delta\chi$, where $\delta\chi = \tilde{\chi} \exp(j\omega t)$. The governing equations, as described in table 1, therefore can be split into a set of dc equations for the steady-state variables $\bar{\chi}$ and a similar set of ac equations for the time-independent, frequency-

[†] Strictly speaking, one takes the real part of such complex expressions: $\chi = \bar{\chi} + \text{Re} \{ \tilde{\chi} \exp(j\omega t) \}$.

domain phasors, $\tilde{\chi}$.

The steady-state form of the equations found in table 1 has been solved by Pollard and Newman,^[11] without including the effect of migration. For the problem at hand, the set of steady-state equations ($\partial c_i/\partial t = 0$) can be cast into a one-dimensional, finite-difference form and resolved using Newman's BAND and MATINV^[2] subroutines, with the appropriate boundary conditions given in table 4.

An iterative procedure is necessary for the solution to the steady-state problem, and therefore initial guesses for the concentration and potential profiles are required. Thus, the supporting electrolyte species profiles are assumed to be equal to their bulk concentrations. The minor species, however, typically vary rather significantly across the boundary layer. For a metal dissolution reaction, the concentration profile of the product species is assumed to take the form

$$\bar{c}_P(z) = \bar{c}_{P,0} \exp\left(-\frac{z}{\delta_P}\right) \quad \text{and} \quad \bar{c}_{i,0} = \bar{c}_{i,\infty} - \frac{s_i \bar{i}_f}{n F} \frac{\bar{\delta}_i}{D_i} \quad (10)$$

The Nernst diffusion-layer thickness, $\bar{\delta}_i = \Gamma(4/3) \delta_i$, was given earlier in the paper. Finally, the kinetic expression given in table 4 is simplified, specifically for a metal dissolution reaction, to

$$\frac{\bar{i}_f}{n F} = \frac{k_a \exp\left(\frac{\alpha_a F}{RT} \bar{V}\right) - k_c \bar{c}_{P,\infty} \exp\left(\frac{-\alpha_c F}{RT} \bar{V}\right)}{1 + \frac{\bar{\delta}_P}{D_P} k_c \exp\left(\frac{-\alpha_c F}{RT} \bar{V}\right)}, \quad (11)$$

where the surface concentration $\bar{c}_{P,0}$ has been eliminated from the equation using the Nernst diffusion-layer approximation.

The set of governing equations in table 1 is changed from the time domain to the frequency domain by replacing $\partial c_i / \partial t$ with $j\omega\tilde{c}_i$. Then the complex potential and concentration phasors, represented by $\tilde{\chi} = \text{Re} \{ \tilde{\chi} \} + j \text{Im} \{ \tilde{\chi} \}$, are split into their real and imaginary parts, yielding twice as many, frequency-coupled linear equations. Linearity makes the numerical computation of the ac problem simpler; furthermore, the finite-difference matrix of coefficients (see appendix of reference 2) is identical to that for the properly linearized dc part except for the additional terms arising from the time derivatives.

4. Total Impedance

Let us now turn our attention to the determination of the total electrochemical impedance. The governing equations in the Stefan-Maxwell model, described above, can be solved numerically yielding the real and the imaginary parts of the concentrations and the potential, which in turn can be used to determine the complex impedance using the following expression:

$$Z_{tot} = \frac{\tilde{V} + (\tilde{\Phi}_0 - \tilde{\Phi}_0)}{i_f + j\omega\tilde{q}} + R_\Omega \quad (12)$$

(An alternative expression for Z_{tot} is given in appendix B in terms of the surface and concentration overpotentials).

The total cell potential V_{tot} is given by equation 7 and consists of three ac components: again, \tilde{V} is the kinetic driving force across the interface, $\tilde{\Phi}_0 - \tilde{\Phi}_0$ is the potential difference across the diffusion layer (and includes the diffusion potential and the ohmic drop due to variations in the conductivity), and the last term in equation 12, the primary solution resistance R_Ω , gives rise to the ohmic potential drop. The liquid-

junction potential has no ac component by definition.

The resulting total alternating current density is the sum of the faradaic current density and the charging current density ($\tilde{i}_c = j\omega\tilde{q}$ replaces $\partial q/\partial t$). The ac faradaic current density, $\tilde{i}_f = \sum_l \tilde{i}_{f,l} = F \sum_i z_i \tilde{N}_i^{(cl)}$, is a function of the kinetic potential difference \tilde{V} and the time-independent alternating part of the concentration $\tilde{c}_{i,0}$ of all species just outside the diffuse part of the double layer. Linearization of the modified Butler-Volmer rate equation given in table 4 using a Taylor expansion around the steady-state values of $\bar{c}_{i,0}$ and \bar{V} yields

$$\tilde{i}_{f,l} = \left(\frac{\partial i_{f,l}}{\partial V} \right)_{c_i} \Big|_{\bar{c}_{i,0}, \bar{V}} \tilde{V} + \sum_i \left(\frac{\partial i_{f,l}}{\partial c_i} \right)_{V} \Big|_{\bar{c}_{i,0}, \bar{V}} \tilde{c}_{i,0} \quad (13)$$

The partial derivatives are functions of the kinetics of reaction l . Therefore, they cannot be determined until a specific reaction mechanism is chosen for the given electrochemical system.

The alternating charge density, \tilde{q} , can be determined using a Taylor series similar to equation 13 for $\tilde{i}_{f,l}$

$$\tilde{q} = \left(\frac{\partial q}{\partial V} \right)_{c_i} \Big|_{\bar{c}_{i,0}, \bar{V}} \tilde{V} + \sum_i \left(\frac{\partial q}{\partial c_i} \right)_{V} \Big|_{\bar{c}_{i,0}, \bar{V}} \tilde{c}_{i,0} \quad (14)$$

where \tilde{q} is a function of the potential difference \tilde{V} and the concentrations $\tilde{c}_{i,0}$. The differential double-layer capacity C is defined by the first partial derivative on the right, where both partial derivatives in equation 14 are functions of the double-layer structure and cannot be determined until a detailed microscopic model^[16] of the interface is specified. However, the purpose of this paper is to present a macroscopic framework for

the electrochemical impedance; thus, a complex model of the double layer, *e.g.*, the work of Appel,^[17] accounting for the effect that concentration variations have on the diffuse layer, is not incorporated in the present treatment. Instead, linearized diffuse-layer theory (see appendix A) can be applied.

The complex impedance can be obtained after multiplying equation 8 by the complex conjugate of the current density, \tilde{i}^* , which yields the following generalized form of the real and the imaginary parts of the total impedance:

$$\operatorname{Re} \{ Z_{tot} \} = \frac{\operatorname{Re} \{ \tilde{V}_{tot} \} \operatorname{Re} \{ \tilde{i} \} + \operatorname{Im} \{ \tilde{V}_{tot} \} \operatorname{Im} \{ \tilde{i} \}}{\operatorname{Re}^2 \{ \tilde{i} \} + \operatorname{Im}^2 \{ \tilde{i} \}} \quad (15)$$

and

$$\operatorname{Im} \{ Z_{tot} \} = \frac{\operatorname{Re} \{ \tilde{i} \} \operatorname{Im} \{ \tilde{V}_{tot} \} - \operatorname{Im} \{ \tilde{i} \} \operatorname{Re} \{ \tilde{V}_{tot} \}}{\operatorname{Re}^2 \{ \tilde{i} \} + \operatorname{Im}^2 \{ \tilde{i} \}} \quad (16)$$

Let us now briefly discuss the components of the total impedance that are contained within equation 12 for Z_{tot} .

Historically, the faradaic impedance is defined by $Z_f = \tilde{V} / \tilde{i}_f$ and is the kinetic contribution to the total impedance accounting for variations in the surface concentrations of all species in solution. The solution impedance, $Z_{soln} = (\tilde{\Phi}_0 - \tilde{\Phi}_0) / \tilde{i} + R_\Omega$, arises from the potential difference across the diffusion layer and consists of two terms. The first results from the establishment of a diffusion potential and ohmic drop (accounting for the variable conductivity) due to concentration gradients across the diffusion layer. This term is typically neglected in other ac-impedance treatments. The second contribution to Z_{soln} , R_Ω , is the ohmic resistance given by equation 6.

5. Conclusions

In this paper, we have presented a macroscopic model for electrode kinetics and electrolytic mass transfer adjacent to a rotating disk. Additionally, the governing equations associated with the total impedance of a given electrochemical system have been discussed. The theoretical treatment accounts for concentrated-solution theory, incorporating the Stefan-Maxwell multicomponent transport equations, and an arbitrary number of homogeneous and heterogeneous reactions, as well as a finite Schmidt number and interfacial velocity. Detailed breakdowns of the various potentials were included in the text and in appendix B. This approach gives rise to impedance terms typically neglected in other theoretical treatments of the impedance. Thus, this work makes it possible to see where certain assumptions have been made in the electrochemical literature. It is hoped that this analysis will help clarify the impedance definitions that are sometimes confusing and not universally recognized.

The model presently does not account for porous salt or oxide films at the electrode surface or specific adsorption, although incorporation of linearized diffuse double-layer theory into the electrode boundary condition is discussed in appendix A. In future papers, the Stefan-Maxwell model is to be used to predict the frequency-response of a copper rotating disk, a system that does not have surface films or a significant amount of specifically adsorbed ions.

Acknowledgements

This work was supported by the Assistant Secretary for Conservation and Renewable Energy, Office of Energy Storage and Distribution, Energy Storage Division, of the U.S. Department of Energy under Contract No. DE-AC03-76SF00098.

Appendix A. The Linearized Diffuse-Layer Boundary Condition

The governing equations within the electrical double layer serve as the electrode boundary condition to the macroscopic problem discussed in this paper. A simplified theoretical framework for the case of no specific adsorption is presented here, although a microscopic model^[18] of the double layer is necessary to describe the detailed electrode-electrolyte interfacial phenomena. The double layer and the mass-transport boundary layer are shown schematically in figure 2. The concept of separating the diffusion layer and the double layer has been rigorously justified by Newman^[19] using a perturbation analysis.

The double layer is the small region, enclosed by $y = 0$ and $z = 0$, where a large electric field and a nonzero charge density exist. The outer Helmholtz plane (OHP), denoted by y_2 , is the plane of closest approach of nonspecifically adsorbed ions and splits the double layer into two regions: the inner or compact region and the diffuse layer. The potential difference across the double layer, $V = \Phi_m - \Phi_0$, can be split according to

$$V = V' + (\Phi_2 - \Phi_0) \quad , \quad (\text{A1})$$

where $V' = \Phi_m - \Phi_2$ is the Frumkin^[20] corrected kinetic potential driving force. When the potential at the OHP, Φ_2 , is small such that $\frac{\Phi_2 - \Phi_0}{RT/F} \ll 1$, linearized diffuse-layer theory can be used. Therefore, the capacity of the diffuse layer, defined by $C_d = -(\partial q_2 / \partial \Phi_2)$, can be approximated by

$$C_d = \frac{-q_2}{\Phi_2 - \Phi_0} \quad (\text{A2})$$

The diffuse charge density q_2 accumulates due to adsorbed ions in the diffuse part of the double layer and is related to the surface concentrations of these species by

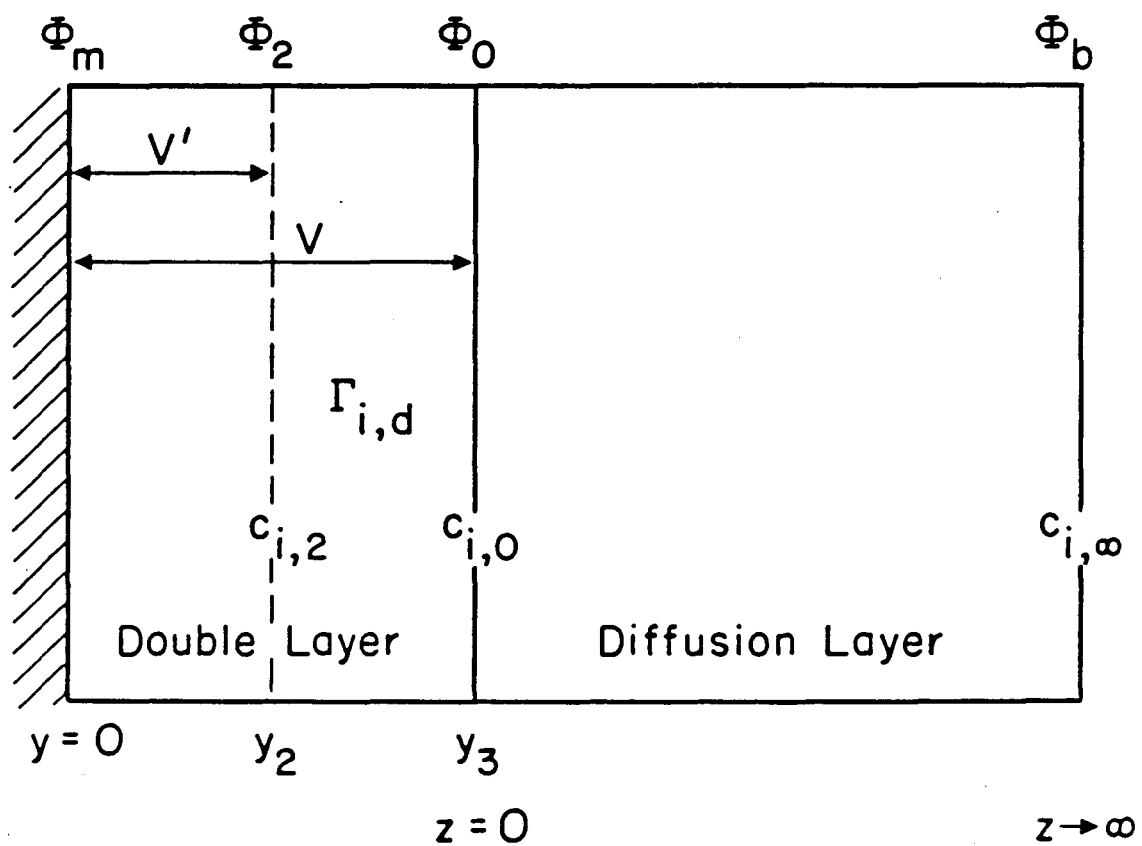


Figure 2. Schematic of the double layer without specific adsorption.

$$q_2 = F \sum_i z_i \Gamma_{i,d} \quad (\text{A3})$$

The material balance for a species within the diffuse layer was given in table 4

$$\frac{\partial \Gamma_{i,d}}{\partial t} = N_i^{(ct)} - N_i(\xi = 0) \quad , \quad (\text{A4})$$

where the fluxes $N_i^{(ct)}$ and $N_i(0) = J_i(0) + c_{i,0}v_0$ were discussed in the text. Here, we present linearized diffuse-layer theory for no specific adsorption that enables $\Gamma_{i,d}$ to be characterized in terms of the variables used in the macroscopic model, V and $c_{i,0}$.

The surface concentration $\Gamma_{i,d}$ of species i in the diffuse layer is defined by

$$\Gamma_{i,d} = \int_{y_2}^{y_3} (c_i - c_{i,0}) dy = c_{i,0} \int_{y_2}^{y_3} \left(\frac{-z_i F}{RT} \Phi \right) dy \quad (\text{A5})$$

where a linearized form of the Boltzmann distribution

$$c_i(y) = c_{i,0} \exp \left(\frac{-z_i F}{RT} \Phi(y) \right) \quad (\text{A6})$$

is used to obtain the right side of equation A5. The position y_3 is equivalent to $z = 0$, the inner limit of the diffusion layer.

The determination of the potential as a function of distance is possible using equation 52-10 in reference [2]

$$y - y_2 = \int_{\Phi}^{\Phi_2} \frac{d\Phi}{E} = \lambda \ln \frac{\Phi_2}{\Phi} \quad , \quad (\text{A7})$$

where E is given as a function of Φ by equation 52-8. The resulting equation on the right is obtained by linearizing E . The Debye length λ characterizes the thickness of the diffuse layer and is given by

$$\lambda = \left(\frac{\epsilon RT}{F^2 \sum_i z_i^2 c_{i,0}} \right)^{1/2}, \quad (\text{A8})$$

where ϵ is the permittivity. Rearrangement of equation A7 yields

$$\Phi = \Phi_2 e^{-(y-y_2)/\lambda}, \quad (\text{A9})$$

such that the integral in equation A5 can now be evaluated. The resulting surface concentration is given by

$$\Gamma_{i,d} = -z_i c_{i,0} \lambda \frac{F \Phi_2}{RT}. \quad (\text{A10})$$

Equation A3 for the charge in the diffuse layer can be rewritten

$$q_2 = -\lambda \frac{F^2 \Phi_2}{RT} \sum_i z_i^2 c_{i,0}. \quad (\text{A11})$$

Elimination of Φ_2 between equations A10 and A11 yields

$$\Gamma_{i,d} = \frac{z_i c_{i,0}}{F \sum_j z_j^2 c_{j,0}} q_2 = z_i c_{i,0} \frac{\lambda^2}{\epsilon} \frac{F q_2}{RT}. \quad (\text{A12})$$

The definition of the Debye length (equation A8) is used to obtain the second expression on the right.

The interfacial region as a whole is electrically neutral; thus, with no specific adsorption, $q_2 = -q$, where q is the charge density that exists on the metal side of the interface. Gauss's law can be written at the metal side of the interface yielding

$$q = \frac{\epsilon_{M-2}}{y_2} (\Phi_m - \Phi_2) = C_{M-2} V', \quad (\text{A13})$$

where C_{M-2} is the capacitance of the inner part of the double layer. Substitution of equations A2 and A13 into equation A1, with rearrangement, yields

$$q = \left(\frac{1}{C_{M-2}} + \frac{1}{C_d} \right)^{-1} V. \quad (\text{A14})$$

Finally, the surface concentration given by equation A12 can be rewritten

$$\Gamma_{i,d} = -z_i c_{i,0} \frac{\lambda^2}{\epsilon} \frac{FV}{RT} \left(\frac{1}{C_{M-2}} + \frac{1}{C_d} \right)^{-1} \quad (\text{A15})$$

giving the necessary equation for treating ion adsorption within the diffuse part of the double layer. This equation, in turn, couples the transient macroscopic mass-transfer and kinetic problem.

Appendix B. Alternative Breakdown of the Total Impedance

An alternative to the total impedance Z_{tot} is obtained by breaking down the potential V_{tot} as follows:^[21]

$$V_{tot} = (\Phi_m - \Phi_{S,0}) + (\Phi_{S,0} - \hat{\Phi}_{S,0}) + (\hat{\Phi}_{S,0} - \Phi_{S,b}) + (\Phi_{S,b} - \Phi_{RR}), \quad (\text{B1})$$

where Φ_S is the potential of a reference electrode of the same type as the working electrode reaction l . The subscripts 0 and b refer to the position just outside the diffuse layer and in the bulk, respectively. $\hat{\Phi}_{S,0}$ is similar to the potential $\hat{\Phi}_0$ defined in the text, but is determined in the absence of concentration gradients by a reference electrode of the same kind as the working electrode, as opposed to a reference electrode of a given kind.

Newman^[2] defines the total overpotential at the electrode as

$$\eta_l = \Phi_m - \hat{\Phi}_{S,0} = \eta_{s,l} + \eta_{c,l} \quad (\text{B2})$$

This is the sum of the first two terms on the right in equation B1. The surface overpotential, $\eta_{s,l} = \Phi_m - \Phi_{S,0}$, is associated with the heterogeneous electrode reaction l , and the concentration overpotential, $\eta_{c,l} = \Phi_{S,0} - \hat{\Phi}_{S,0}$, is associated with concentration changes in the diffusion layer.

The total cell potential given by equation B1 can be rewritten

$$V_{tot} = \eta_{s,l} + \eta_{c,l} + \Delta\hat{\Phi}_{ohm} + U_{i/RR}'' \quad (\text{B3})$$

where each of these potential differences is illustrated in figure 3. It should be pointed out that one should be careful when a reactant or product is absent in the bulk solution since then $\eta_{c,l}$ and $U_{i/RR}''$ go to plus and minus infinity in a way that their sum remains finite. For such a case, the previous breakdown of potential (given by equation 7 in the text) should be applied since it avoids this problem.

$\Delta\hat{\Phi}_{ohm} = \hat{\Phi}_{S,0} - \Phi_{S,b} = iR_{\Omega}$ is the ohmic drop from the electrode surface to the bulk solution, when there are no concentration variations, and R_{Ω} again is the calculated primary resistance. The last term in equation B3 is the cell potential of reaction l relative to a real reference electrode,

$$U''_{i/RR} = (\Phi_{S,b} - \Phi_b) + (\Phi_b - \Phi_{RR}) = U'_{i/RG,\infty} + \Delta\Phi_{LJ} \quad (B4)$$

and contains both a thermodynamic and a junction potential. The thermodynamic cell potential of reaction l relative to a given reference electrode[†] is given by

$$U'_{i/RG} = U_i^{\theta} - U_{RG}^{\theta} + \frac{RT}{F} \ln \frac{c_{Cl^-,sat}}{\rho_0} - \frac{RT}{n_l F} \sum_i s_{i,l} \ln \left(\frac{c_i \int_{i,Cl^-}}{\rho_0} \right), \quad (B5)$$

where the reference electrode of a given kind is specified to be a saturated (4.1 M) calomel electrode. Additionally, the first three terms in this expression yield the thermodynamic equilibrium constant $\ln K_l$ for an electrochemical reaction and was given in table 5.

The alternating total voltage can be written as

$$\tilde{V}_{tot} = \tilde{\eta}_{s,l} + \tilde{\eta}_{c,l} + \tilde{i} R_{\Omega} + \tilde{U}''_{i/RR}, \quad (B6)$$

where the last term is zero since it has no ac component due to being evaluated at the bulk conditions. This alternative breakdown of the total cell potential is convenient if a Butler-Volmer kinetic expression is used

[†] Using a reference electrode of a given kind lends itself to a thermodynamic equilibrium potential difference, $U'_{i/RG}$, (denoted by a single prime) because any liquid-junction potential which might exist between the solution in question and that within the reference-electrode compartment is corrected for by definition of the ideal reference electrode. "Corrected for liquid-junction potentials" means making the requirement that the electrical states of the two solutions be equal.^{[2],[18]}

$$i_{f,l} = i_{0,l} \left[\exp \left(\frac{\alpha_a F}{RT} \eta_{s,l} \right) - \exp \left(- \frac{\alpha_c F}{RT} \eta_{s,l} \right) \right], \quad (\text{B7})$$

where $i_{0,l}$ is the exchange current density and is given by

$$i_{0,l} = n_l F k_{f,l}^{(\frac{\alpha_c}{\alpha_a + \alpha_c})} k_{b,l}^{(\frac{\alpha_a}{\alpha_a + \alpha_c})} \prod_i c_{i,0}^{(\frac{\alpha_c}{\alpha_a + \alpha_c})} \prod_i c_{i,0}^{(\frac{\alpha_a}{\alpha_a + \alpha_c})} \quad (\text{B8})$$

$$s_{i,l} > 0 \quad s_{i,l} < 0$$

This equation is obtained by setting $i_{f,l} = 0$ in table 5 in the text and noting that $V = \eta_{s,l} + U_{l/RG,0}^j$. Linearization of the Butler-Volmer equation B7 with respect to $\eta_{s,l}$ and $c_{k,0}$ yields the alternating faradaic current density. The resulting expression for \tilde{i}_f is similar to equation 13 in the text for a modified Butler-Volmer kinetic expression.

Finally, the total impedance can be rewritten

$$Z_{tot} = \frac{\tilde{\eta}_{s,l} + \tilde{\eta}_{c,l}}{\tilde{i}_f + j\omega\tilde{q}} + R_\Omega, \quad (\text{B9})$$

and should be compared to equation 12 in the text for Z_{tot} . It should be pointed out that the convective-Warburg impedance Z_W given by Homay *et al.*^[22] is

$$Z_W = \frac{\tilde{\eta}_{c,l}}{\tilde{i}_f} = \sum_i \left(\frac{s_{i,l}}{n_l F} \right)^2 \left(\frac{\nu}{\Omega} \right)^{1/2} \left(\frac{3D_i}{a\nu} \right)^{1/3} \frac{RT}{\bar{c}_{i,0} D_i} \left\{ \frac{-1}{\theta'(0)} \right\}, \quad (\text{B10})$$

which is valid for dilute solutions, no migration, and an infinite Schmidt number.

Double-layer-charging effects are not included in the definition of Z_W .

List of Symbols

a	0.51023
b	-0.61589
c_T	total solution concentration, including the solvent, mol/cm ³
c_i	concentration of species i , mol/cm ³
$c_{i,0}$	concentration of species i at the electrode surface, mol/cm ³
$c_{i,\infty}$	bulk concentration of species i , mol/cm ³
\bar{c}_i	steady-state concentration of species i , mol/cm ³
\tilde{c}_i	alternating concentration phasor of species i , mol/cm ³
C_{M-2}	capacitance of the compact region of the double-layer, F/cm ²
C_d	capacitance of the diffuse part of the double layer, F/cm ²
C_{dl}	integral double-layer capacitance, F/cm ²
C	differential double-layer capacitance, F/cm ²
D_i	dilute-solution diffusion coefficient of species i , cm ² /s
$D_{i,k}$	diffusion coefficient for interaction of species i and k , cm ² /s
e^-	symbol for the electron
$f_{i,n}$	molar activity coefficient of species i relative to species n
F	Faraday's constant, 96,487 C/equiv
i	current density, A/cm ²
\bar{i}	steady-state current density, A/cm ²
$ \tilde{i} $	amplitude of current perturbation, A/cm ²

i_f	total faradaic current density of reaction l , A/cm ²
$i_{f,l}$	faradaic current density of reaction l , A/cm ²
$\tilde{i}_{f,l}$	alternating faradaic current density of reaction l , A/cm ²
\tilde{i}_f	alternating total faradaic current density, A/cm ²
i_0	exchange current density, A/cm ²
j	$= \sqrt{-1}$, imaginary number
J_i	molar flux relative to the mass-average velocity, mol/cm ² ·s
k_a, k_c	anodic and cathodic rate constant for a charge transfer reaction, variable units
$k_{f,l}, k_{b,l}$	forward and back rate constant for heterogeneous reaction l , variable units
$\hat{k}_{f,l}, \hat{k}_{b,l}$	forward and back rate constant for homogeneous reaction l , variable units
K_l	thermodynamic equilibrium constant for electrochemical reaction l , (mol/kg) ^{-ν_l}
$K_{c,l}$	concentration thermodynamic equilibrium constant for electrochemical reaction l , (mol/cm ³) ^{-ν_l}
\hat{K}_l	thermodynamic equilibrium constant for homogeneous reaction l , (mol/kg) ^{-ν_l}
$\hat{K}_{c,l}$	concentration thermodynamic equilibrium constant for homogeneous reaction l , (mol/cm ³) ^{-ν_l}
m_i	molality of species i , mol/kg
M_i	molecular weight of species i , g/mol
\bar{M}	average molecular weight of the solution, weighted by mole fractions and including the solvent, g/mol
n_l	number of electrons involved in electrode reaction l

$N_i^{(ct)}$	molar flux of species i through the interface due to electrochemical charge-transfer reactions, mol/cm ² ·s
r_0	radius of disk electrode, cm
r_l	rate of heterogeneous reaction l , mol/cm ² ·s
R	universal gas constant, 8.3143 J/mol·K
R_i	rate of homogeneous production of species i , mol/cm ³ ·s
\hat{R}_l	rate of homogeneous reaction l , mol/cm ³ ·s
R_s	experimental solution resistance obtained from the infinite-frequency limit of the total impedance, ohm·cm ²
R_Ω	primary solution resistance, ohm·cm ²
R'_Ω	calculated effective solution resistance, ohm·cm ²
R_t	charge-transfer resistance, ohm·cm ²
R_0	low-frequency limit of the mass-transfer impedance Z_0 , ohm·cm ²
$s_{i,l}$	stoichiometric coefficient of species i in electrode reaction l
s_l	stoichiometric coefficient parameter for electrode reaction l
Sc	Schmidt number
t	time, s
t_i^0	transference number of species i with respect to the velocity of the solvent
T	absolute temperature, K
U_l^θ	standard thermodynamic potential of reaction l relative to the standard hydrogen reference electrode, V
$U_{l/RG}^\theta$	standard thermodynamic potential difference between reaction l and the reference electrode reaction of a given kind RG , V

$U'_{i/RG}$	thermodynamic cell potential difference between reaction l and a reference electrode reaction of a given kind RG , V
$U''_{i/RR}$	cell potential difference between reaction l and the real reference electrode reaction RR , V
v	mass-average velocity, cm/s
v_i	velocity of species i , cm/s
v_0	velocity through the interface, cm/s
v_z	normal velocity for rotating disk, cm/s
V	kinetic driving force (electrode potential relative to given reference electrode placed just outside double layer), V
\bar{V}	steady-state part of kinetic potential driving force, V
$ \tilde{V} $	amplitude of the potential perturbation relative to given reference electrode, V
V_{tot}	total cell potential (electrode potential relative to a real reference electrode placed in the bulk solution), V
\bar{V}_{tot}	steady-state part of total cell potential, V
$ \tilde{V}_{tot} $	amplitude of the potential perturbation relative to a real reference electrode, V
x_0	mole fraction of solvent water
x_i	mole fraction of species i
y	normal distance from surface in double layer, cm
y_2	position at outer Helmholtz plane
z	normal distance from surface in transport boundary layer, cm
z_i	charge number of species i
Z_{tot}	complex total electrochemical impedance, ohm-cm ²
Z_{soln}	complex solution impedance, ohm-cm ²

Z_f	complex faradaic impedance, ohm-cm ²
Z_0	complex mass-transfer part of faradaic impedance, ohm-cm ²
Z_W	complex convective-Warburg impedance, ohm-cm ²

Greek symbols:

$\alpha_{a,l}$	anodic transfer coefficient for reaction l
$\alpha_{c,l}$	cathodic transfer coefficient for reaction l
β_l	symmetry factor for reaction l
Γ_i	surface concentration of species i , mol/cm ²
$\Gamma_{i,d}$	surface concentration of species i in the diffuse layer, mol/cm ²
$\Gamma(4/3)$	0.89298, the gamma function of 4/3
δ_i	scaling factor for the diffusion layer of species i , cm
$\bar{\delta}_i$	Nernst diffusion-layer thickness for species i , cm
ΔG_l^θ	standard Gibbs free energy of formation for homogeneous reaction l , J/mol
$\Delta\Phi_{LJ}$	liquid-junction potential, V
$\Delta\hat{\Phi}_{ohm}$	ohmic potential drop, V
ϵ_{M-2}	permittivity within the inner part of the double layer, F/cm or C/V·cm
ϵ	permittivity within the diffuse double layer, F/cm or C/V·cm
ζ	dimensionless axial distance for rotating disk
$\tilde{\eta}_{s,l}$	complex, time-independent phasor of the surface overpotential, V

$\tilde{\eta}_{c,l}$	complex, time-independent phasor of the concentration overpotential, V
$-1/\theta'(0)$	complex, dimensionless, convective-Warburg impedance function
κ	conductivity, $\text{ohm}^{-1}\cdot\text{cm}^{-1}$
λ	Debye thickness of the diffuse double layer, cm
μ_i	electrochemical potential of species i , J/mol
ν	kinematic viscosity, cm^2/s
ρ_0	density of pure solvent, g/cm^3
ρ'_0	density of pure solvent, kg/cm^3
ξ_i	dimensionless axial distance for rotating-disk convective-diffusion equation for species i
ξ_R	dimensionless axial distance for rotating-disk convective-diffusion equation for the reference species R
ξ_{\max}	dimensionless boundary-layer thickness for rotating-disk
π	3.141592654
ϕ	phase angle
Φ	electrostatic potential, V
Φ_m	potential of the metal electrode, V
Φ_S	potential of a reference electrode of the same kind as the working electrode, V
$\hat{\Phi}_{S,0}$	potential of a reference electrode of the same kind as the working electrode placed just outside the double layer as if there were no concentration gradients across the boundary layer, V

Φ_{RG}	potential of a hypothetical reference electrode of a given kind, V
Φ_0	potential of a hypothetical reference electrode of a given kind placed just outside the double layer, V
$\hat{\Phi}_0$	potential of a reference electrode of a given kind placed just outside the double layer as if there were no concentration gradients across the boundary layer, V
Φ_2	potential of a hypothetical reference electrode of a given kind placed at the outer Helmholtz plane of the double layer, V
Φ_b	potential of a hypothetical reference electrode of a given kind placed in the bulk of the solution, V
Φ_{RR}	potential of a real reference electrode placed in the bulk of the solution, V
χ	dummy variable
$\bar{\chi}$	steady-state part of χ
$\delta\chi$	complex, time-dependent part of χ
$\tilde{\chi}$	complex, time-independent phasor of χ
$ \tilde{\chi} $	amplitude of perturbation χ
Ψ	dimensionless set potential
ω	perturbation frequency, rad/s
Ω	angular rotation speed of disk, rad/s

subscripts:

a	anodic
b	back reaction

<i>c</i>	cathodic
<i>f</i>	forward reaction
<i>m</i>	at the metal electrode surface
<i>2</i>	in the diffuse part of the double layer
<i>0</i>	just outside the diffuse part of the double layer
<i>b</i>	in the bulk electrolyte, where there are no concentration variations
∞	in the bulk electrolyte, where there are no concentration variations
<i>LJ</i>	liquid junction
<i>R</i>	principal reactant
<i>RG</i>	reference electrode of a given kind
<i>RR</i>	real reference electrode placed in the bulk solution
<i>S</i>	reference electrode of the same kind as the working electrode

superscripts:

—	time-average or steady-state part
~	complex, time-independent part
^	assumes constant conductivity equal to that in the bulk electrolyte

References

- [1]. Bernard Tribollet and John Newman, "Impedance Model for a Concentrated Solution. Application to the Electrodeposition of Copper Solutions," *Journal of the Electrochemical Society*, *131*, 2780-2785 (1984).
- [2]. John Newman, *Electrochemical Systems*, Englewood Cliffs, N. J.: Prentice-Hall, Inc., 1973.
- [3]. Th. V. Kármán, "Über laminare und turbulente Reibung," *Zeitschrift für angewandte Mathematik und Mechanik*, *1*, 233-252 (1921).
- [4]. W. G. Cochran, "The flow due to a rotating disc," *Proc. Cambridge Phil. Soc.*, *30*, 365 (1934).
- [5]. Ralph White, Charles M. Mohr, Jr., and John Newman, "The Fluid Motion to a Rotating Disk," *Journal of the Electrochemical Society*, *123*, 383-385 (1976).
- [6]. Veniamin G. Levich, *Physicochemical Hydrodynamics*, Englewood Cliffs, N. J.: Prentice-Hall, Inc., 1962.
- [7]. L. Hsueh and J. Newman, "Mass Transfer and Polarization at a Rotating Disk Electrode," *Electrochimica Acta*, *12*, 429-438 (1967).
- [8]. John Newman, "Current Distribution on a Rotating Disk below the Limiting Current," *Journal of the Electrochemical Society*, *113*, 1235-1241 (1966).
- [9]. John Newman, "Frequency Dispersion in Capacity Measurements at a Disk Electrode," *Journal of the Electrochemical Society*, *117*, 198-203 (1970).

- [10]. J. Newman and L. Hsueh, "The Effect of Variable Transport Properties on Mass Transfer to a Rotating Disk," *Electrochimica Acta*, *12*, 417-427 (1967).
- [11]. Richard Pollard and John Newman, "Silicon Deposition on a Rotating Disk," *Journal of the Electrochemical Society*, *127*, 744-749 (1980).
- [12]. Klaus J. Vetter, *Electrochemical Kinetics, Theoretical and Experimental Aspects*, New York: Academic Press Inc., 1967.
- [13]. P. Henderson, "Zur Thermodynamik der Flüssigkeitsketten," *Zeitschrift für physikalische Chemie*, *59*, 118-127 (1907).
- [14]. William H. Smyrl and John Newman, "Potentials of Cells with Liquid Junctions," *Journal of Physical Chemistry*, *72*, 4660-4671 (1968).
- [15]. John Newman, "Resistance for Flow of Current to a Disk," *Journal of the Electrochemical Society*, *113*, 501-502 (1966).
- [16]. Alan K. Hauser and John Newman, "A Microscopic Impedance Model of the Electrode/Electrolyte Interface. Adsorption Mechanism for Zinc Dissolution in Chloride Solutions," Abstract 251, Fall ECS Meeting, Honolulu, 1987.
- [17]. Peter Appel, Ph.D. thesis, University of California, Berkeley, CA, LBL-532, May, 1976.
- [18]. Alan K. Hauser and John Newman, "A Microscopic-Impedance Model for a Rotating Disk Electrode," LBL-26268, submitted to *Journal of the Electrochemical Society* (1989).

- [19]. John Newman, "The Polarized Diffuse Double Layer," *Transactions of the Faraday Society*, 61, 2229-2237, (1965).
- [20]. A. Frumkin, "Wasserstoffüberspannung und Struktur der Doppelschicht," *Zeitschrift für physikalische Chemie*, 164, 121-133 (1933).
- [21]. Alan K. Hauser, M.S. thesis, University of California, Berkeley, CA, LBL-17461, April, 1984.
- [22]. Robert V. Homsy and John Newman, "An Asymptotic Solution for the Warburg Impedance of a Rotating Disk Electrode," *Journal of the Electrochemical Society*, 121, 521-523 (1974).

LAWRENCE BERKELEY LABORATORY
TECHNICAL INFORMATION DEPARTMENT
1 CYCLOTRON ROAD
BERKELEY, CALIFORNIA 94720